

Simultaneous solar laser emissions from three Nd:YAG rods within a single pump cavity

Dawei Liang^a, Joana Almeida^a, Dário Garcia^a, Bruno D. Tibúrcio^a, Emmanuel Guillot^b, Cláudia R. Vistas^a

^a CEFITEC, Departamento de Física, FCT, Universidade NOVA de Lisboa, 2829-516 Campus de Caparica, Portugal

^b PROMES-CNRS, 7 rue du Four Solaire, 66120, Font Romeu, Odeillo, France

ARTICLE INFO

Keywords

Solar-pumped laser
Laser emission
Multi-rod
Parabolic mirror
Slope efficiency, Nd:YAG

ABSTRACT

We report here, to the best of our knowledge, the first simultaneous emission of three continuous-wave solar laser beams by end-side-pumping three 3.0 mm diameter, 25 mm length Nd:YAG single-crystal rods within a single conical pump cavity. An aspheric fused silica lens was used to couple the concentrated solar radiation from the focal zone of a parabolic mirror with 1.0 m² effective collection area into the laser rods within the pump cavity. 18.3 W multimode solar laser power was measured, resulting in 5.1% laser slope efficiency. 0.036 W laser beam brightness figure of merit was also achieved for each beam, being 9 times more than that of the most efficient solar laser with 32.5 W/m² collection efficiency. Since the three laser rods were associated with their own 1064 nm output mirrors, it was possible to adjust individually both solar laser output power levels and beam qualities of the three laser beams by adopting different resonant cavity lengths, enabling potential solar laser applications.

1. Introduction

Solar-pumped laser is considered as one of the most promising technologies for solar energy research in the 21st century. The direct excitation of renewable lasers by natural sunlight may provide cost-effective solutions to free coherent optical radiation generation, leading to numerous benefits in the years to come. Solar-pumped lasers are usually considered for applications where sunlight is abundant and other forms of energy sources are scarce, especially in space (Vasile and Maddock, 2012; Guan et al., 2017). Powered by free solar energy, solar laser has also large potential for terrestrial applications such as high-temperature materials processing (Yabe et al., 2007).

Since 1966, primary parabolic mirrors have been utilized by Young (Young, 1966) and other researchers (Weksler and Schwartz, 1988; Arashi et al., 1984; Benmair et al., 1990; Lando et al., 2003; Almeida et al., 2013) to achieve tight focusing of incoming solar radiation for the excitation of a laser medium. With secondary and tertiary concentrators, solar laser collection efficiency was gradually boosted to 6.7 W/m² in 2003 (Lando et al., 2003). Significant progresses in solar laser efficiency have been achieved by Fresnel lenses solar laser pumping approaches (Yabe et al., 2007). 18.7 W/m² solar laser collection efficiency, defined as laser output power versus solar collector area, was firstly reported in 2007 by pumping a large Cr:Nd:YAG ceramic laser rod with a 1.4 m² area Fresnel lens (Yabe et al., 2007). 19.3 W/m² laser collection efficiency was later achieved

in 2011 by exciting a 4 mm diameter, 25 mm length Nd:YAG single-crystal rod through a 0.64 m² area Fresnel lens (Liang and Almeida, 2011). This result triggered discussions about which medium between Cr:Nd:YAG ceramics and Nd:YAG single-crystal was more suitable for solar-pumped lasers. Consequently, in 2012, collection efficiency of 30.0 W/m² was attained by pumping a 6 mm diameter, 100 mm length Nd:YAG single-crystal rod through a 4.0 m² area Fresnel lens (Dinh et al., 2012). However, very large $M_x^2 = M_y^2 = 137$ factors were associated with this pumping approach, leading to a low laser beam brightness figure of merit – defined as the ratio between laser power and the product of M_x^2 and M_y^2 (Dinh et al., 2012) – of only 0.0064 W. By end-side-pumping a 4 mm diameter, 35 mm length Nd:YAG single-crystal rod with a heliostat-parabolic mirror solar energy concentration system, 31.5 W/m² multimode solar laser collection efficiency was reported (Liang et al., 2017). Most recently, a monolithic fused silica liquid light guide lens was used to achieve end-side-pumping of a 4.5 mm diameter, 35 mm length Cr:Nd:YAG ceramic laser rod within a conical pumping cavity. 32.5 W/m² solar laser collection efficiency and 6.7% laser slope efficiency were achieved by a parabolic primary mirror. However, large $M_x^2 = M_y^2 = 95$ factors were measured, leading to 0.004 W laser beam brightness figure of merit (Liang et al., 2018).

Manufacturers view laser material processing as a well-understood productivity enhancement, which they constantly seek to extend to new segments of their business. Lately, that search has produced a trend toward the deployment of multiple laser beams on a single work-

E-mail address: dl@fct.unl.pt (D. Liang)

piece, each optimized to perform a facet of the overall process (Strite et al., 17th, 2016.). The following laser beam material processing concepts are usually considered.

1. Single-laser/single-beam concept. It is most commonly used in many laser applications, but can be out of any economic value with the current single spot technology due to the enormous processing time of days and even weeks (Bruening et al., 2018).
2. Multi-laser/multi-beam concept. It is based on macroscopic lateral arrangement of many lasers. A further decrease of the processing time is possible by scaling many single lasers. However, due to the size of the lasers and its beam delivery systems, this approach is limited in the maximum number of deployable laser sources.
3. Single-laser/multi-beam concept based on laser beam splitting technologies. This approach has high compactness because one laser serves all spots. However, laser output power and its beam quality is strongly influenced by the thermal lensing and thermal stress problems of the single-laser source.

To avoid the above mentioned limitations, a single-laser/multi-beam concept based on the simultaneous emissions of multi-beam from a single solar laser is here proposed. This approach has also high compactness since one laser serves all spots. Moreover, the above mentioned thermal lensing and thermal stress problems can be significantly reduced. It can deploy three moderate power renewable laser beams, thus providing the capability to tailor the applied solar laser energy to the specific needs of material processing applications. In some space applications (Guan et al., 2017), the concerns on absolute solar laser power level can be relegated to a less important role, while the simultaneous emissions of several solar laser beams at low power level, but with enhanced beam quality, may become more demanding. It is based on these concerns that the three-rod solar laser scheme was designed, implemented and tested. The design parameters of the three-rod within one pump cavity solar laser system, optimized by ZEMAX© and LASCAD© software, will be explained in Sections 2 and 3. Experiments on continuous-wave three-rod solar laser emissions and three laser beam profiles measurements will then be discussed in Section 4 and 5, finally followed by conclusions in Section 6.

2. Three-rod Nd:YAG solar laser system

2.1. Solar energy collection and concentration system

As shown in Fig. 1, NOVA heliostat-parabolic mirror solar laser system was composed of a large plane mirror (composed of two flat segments) with 93.5% reflectivity, mounted on a two-axis heliostat, which redirected the incoming solar radiation towards a stationary parabolic mirror with 1.5 m diameter, 60° rim angle and 660 mm focal length. The parabolic mirror was back-surface silver coated. Because of

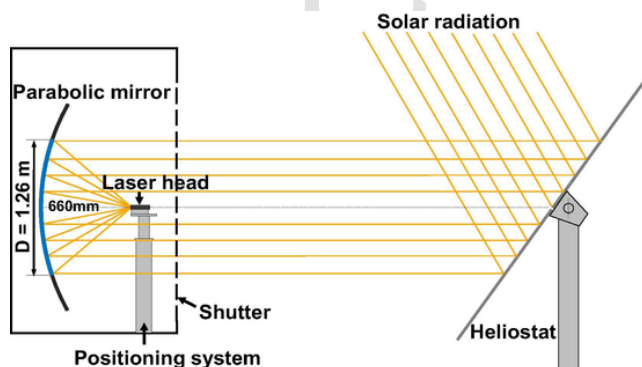


Fig. 1. Schematics of NOVA heliostat - parabolic mirror system for pumping the three-rod solar laser head.

iron impurities within 10 mm glass substrates, 80% reflectivity was measured for this primary mirror. The total combined reflectance of both the heliostat and the parabolic mirror was 74.8%. The input solar power at the focus was limited by masking the external annular area of the 1.5 m diameter mirror, so that only its 1.26 m diameter central circular area was utilized. 1.0 m² effective solar collection area was calculated by discounting the shadowing area of 0.25 m² by the laser head, its supporting mechanics, the X-Y-Z positioner and the non-reflecting space between the two flat segments of the heliostat mirrors.

For a typical solar irradiance of 830 W/m² in Lisbon, September 2019, more than 600 W solar power was focused into a highly concentrated pump light spot with near-Gaussian distribution of 8 mm full width at half maximum (FWHM).

2.2. Solar laser head with the aspheric lens, the three Nd:YAG rods and the single pump cavity

Fig. 2a presents the front image of the solar laser head composed of the large fused silica aspheric lens and the three

3 mm diameter, 25 mm length Nd:YAG rods within the single conical pump cavity. By optically aligning three small partial reflection (PR) 1064 nm output mirrors with their corresponding laser rods, as shown in Fig. 2b, simultaneous cw 1064 nm solar laser emissions were produced. Accurate resonant cavity alignments were ensured by adjusting the output couplers individually through the three positioners. The laser head was fixed on the X-Y-Z axes positioning system, ensuring its optical alignment in the focal zone.

As shown in Figs. 2 and 3, the large fused silica aspheric lens was 84 mm in diameter, 34 mm in thickness, 60 mm in front surface radius of curvature and -0.003 in rear r^2 parameter. The output end face of the lens had a plane surface. The aspheric lens coupled efficiently the concentrated solar radiation from the focal zone into the three Nd:YAG rods. For end-pumping, one part of the concentrated radiation was directly focused onto the high-reflection (HR 1064 nm) end face coatings of the rods by the aspheric lens. The HR coatings reflected the 1064 nm oscillating laser radiation within the resonant cavity, but allowed the passage of other solar pumping wavelengths. For side-pumping, another part of the radiation that did not hit the HR 1064 nm coatings was guided into the conical cavity with

$D_1 = 18$ mm/ $D_2 = 9$ mm input/output diameters and $H_1 = 19$ mm height. The zigzag passage of the rays within the small pump cavity ensured efficient multi-pass side-pumping to the rods. The inner wall of the pumping cavity was bonded with a protected silver-coated aluminum foil with 94% reflectivity. The Nd:YAG rods, the conical pump cavity and the output end face of the aspheric lens were all actively cooled by water at 6 L/min flow rate. The maximum contact between the coolant and the rod was essential for the removal of the generated heat. The central region of the aspheric lens output face was in direct contact with the cooling water, ensuring hence an efficient light coupling of the concentrated solar radiation into the rods. There was 3 mm space between the aspheric lens output end face and the HR1064 nm coatings of the rods, more than enough for the exit of cooling water. Besides, both fused silica material and cooling water were useful for partially preventing both UV solarization and IR heating to the rods. L_1 , L_2 and L_3 represent the laser resonant cavity lengths between the laser rods and their respective PR1064 nm mirrors (PR₁, PR₂ and PR₃).

3. Numerical optimization of the design parameters by ZEMAX© and LASCAD© software

Similar to our previous numerical analysis on solar lasers (Almeida et al., 2013; Liang and Almeida, 2011), all the above mentioned design parameters of the three-rod solar laser system were firstly optimized by non-sequential ray-tracing ZEMAX© software for achieving the maximum absorbed pump power for each of the three rods.

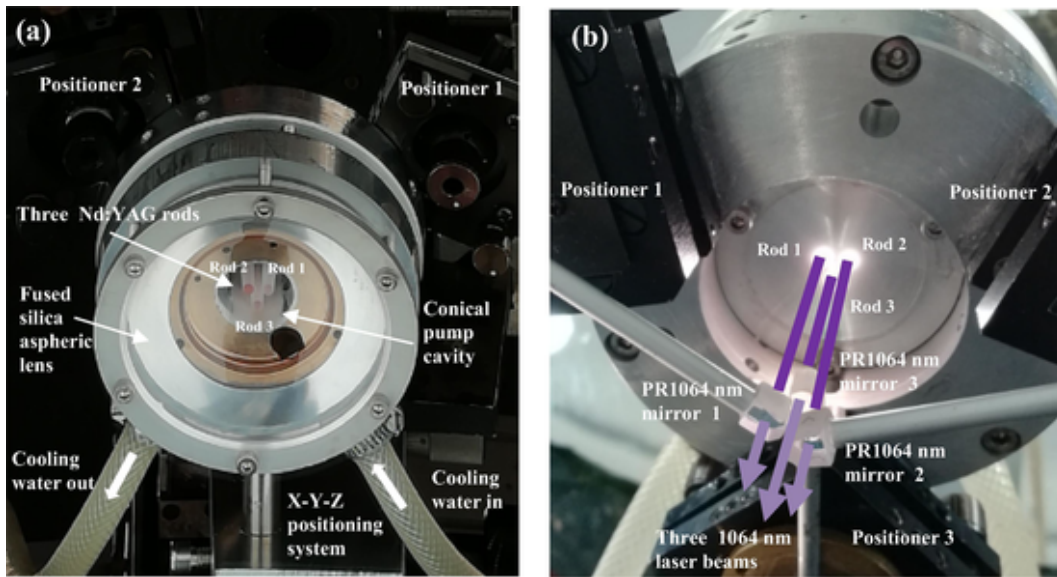


Fig. 2. (a) Front image showing the three-rod solar laser head actively cooled by water. (b) Back image of the solar laser head with three positioners for accurate adjustments of the three small output couplers in relation to the three rods.

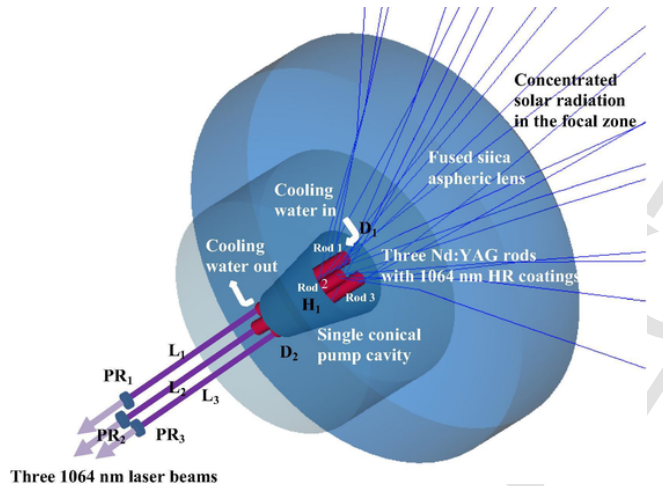


Fig. 3. Design of the three-rod Nd:YAG laser head, composed of the fused silica aspheric lens, the conical pump cavity and the Nd:YAG rods, which were all actively cooled by water.

The pump-flux distributions along longitudinal central cross-sections and five transversal cross-sections of the rods are given in Fig. 4. Red color means near maximum pump absorption, whereas blue means little or no absorption.

Non-uniform distributions along the laser rods were numerically calculated. Nevertheless, these were the distributions that ensured the maximum absorbed pump power by the three rods. During ray-tracing, each 3 mm diameter, 25 mm length active medium was divided into 18,000 zones. The path length in each zone was found. With this value and the effective absorption coefficient of 1.0 at.% Nd:YAG material (Liang and Almeida, 2011), the absorbed power within the laser medium was calculated by summing up the absorbed pump radiation of all zones.

The absorbed pump flux data from the ZEMAX© analysis was then processed by laser cavity analysis and design (LASCAD©) software to optimize solar laser output performances. The stimulated emission cross-section of

$2.8 \times 10^{-19} \text{ cm}^2$, the fluorescence life time of 230 μs and a typical absorption and scattering loss of 0.003 cm^{-1} for the 1.0 at.%

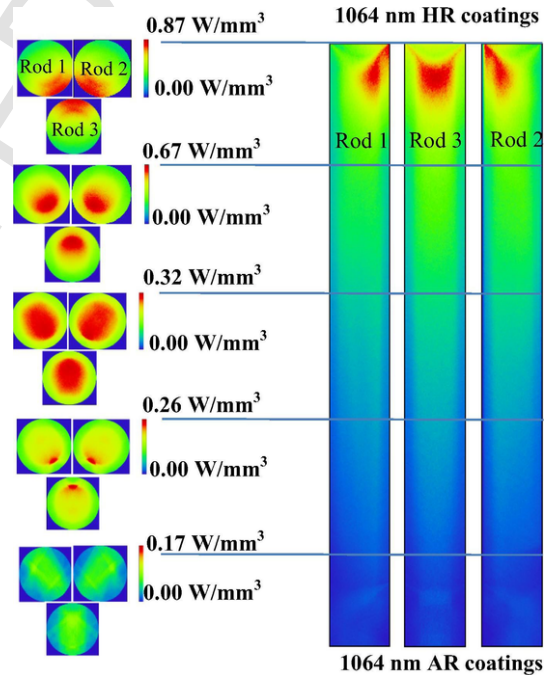


Fig. 4. Absorbed pump-flux distributions along longitudinal central cross-sections and five transversal cross-sections of the three 3 mm diameter, 25 mm length Nd:YAG rods.

Nd:YAG medium were adopted in LASCAD© analysis. The mean absorbed and intensity-weighted solar pump wavelength of 660 nm (Wekler and Schwartz, 1988) was also used in the analysis. L represents the separation length between the output end face anti-reflection (AR) 1064 nm coatings of the Nd:YAG rod and PR1064 nm output mirror, as shown in Fig. 5. L was the key parameter for achieving the highest laser power. PR1064 nm mirrors of different reflectivity (R) and radius of curvature (RoC) were tested individually to optimize laser power for each rod. For the 3 mm diameter, 1.0 at.% Nd:YAG rod with length $L_R = 25 \text{ mm}$, the amount of absorption and scattering losses was $2\alpha L_R = 1.5\%$. Assuming 0.4% of imperfect HR and AR coating losses, the round-trip loss increased to 1.9%. The diffraction losses depend heavily on rod diameter, resonator length and RoC of the resonator mirrors. LASCAD©

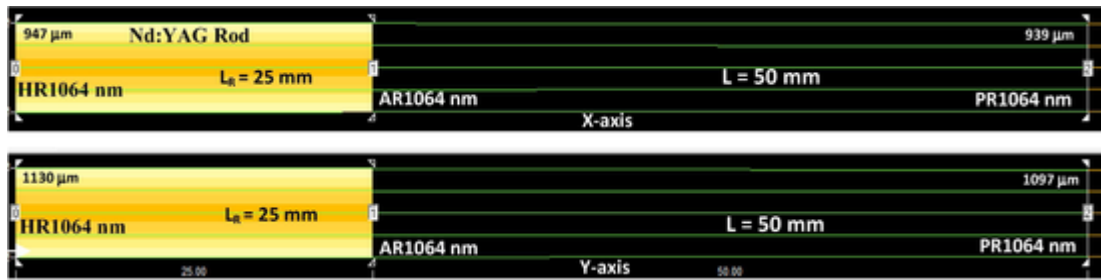


Fig. 5. Laser resonator configuration for the efficient extraction of multimode solar laser power. L represents the separation length between AR1064 nm coating and PR1064 nm mirror.

beam propagation method (BPM) gave 0.05% diffraction loss for $L = 50$ mm and $RoC = \infty$, resulting in a total round-trip loss of 1.95%. Consequently, 6.2 W multimode solar laser power was numerically obtained. The half-widths of the oscillating modes within the resonant cavity (947 μm in X-axis, 1130 μm in Y-axis at HR1064 nm mirror) and (939 μm in X-axis, 1097 μm in Y-axis at PR1064 nm mirror) were also calculated, as shown in Fig. 5. The laser beam quality $M_x^2 = 10.8$, $M_y^2 = 14.7$ factors were then numerically obtained for the PR1064 nm mirror $RoC = \infty$.

In a single-rod solar laser pumping scheme, instead of adopting three 3 mm diameter, 25 mm length Nd:YAG rods within the conical pump cavity in Fig. 3, a 5.2 mm diameter, 25 mm length Nd:YAG rod could also be pumped within the same conical cavity under the same solar pumping conditions as explained in Section 2.2. Since the volume of the 5.2 mm diameter 25 mm length rod was nearly the same as the sum of the volumes of the three 3 mm diameter, 25 mm length rods, the solar laser output performances of both the single-rod and the three-rod solar laser pumping schemes were also analyzed by both ZEMAX© and LASCAD© software, as listed in Table 1.

Due to the gaps between the rods, the three-rod solar laser pumping scheme absorbed 4.7% less solar pump power, and consequently 11% less solar laser power was numerically calculated, as compared to that by the single-rod scheme. Because of the asymmetric and inhomogeneous absorbed pump light distribution along each rod in Fig. 4, the three-rod scheme presented some discrepancies between M_x^2 and M_y^2 factors. The M^2 factors of each laser beam from the three-rod scheme were, however, 2.97 (for M_x^2), 2.18 (for M_y^2) times smaller than that from the single-rod scheme. Consequently, the laser beam brightness figure of merit for each beam was nearly doubled as compared to

that of the single-rod scheme. Besides, the three-rod scheme presented 31.6% reduction in the maximum heat load value as compared to that of the single-rod scheme. It also presented only 303 K maximum temperature value for each rod, which was 22 K less than that of the single-rod Scheme 16.9 N/mm² maximum thermal stress value was calculated for the three-rod scheme, corresponding to 65.5% reduction as compared to that of the single-rod scheme.

4. Simultaneous continuous-wave solar laser emissions from the three Nd:YAG rods

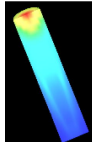
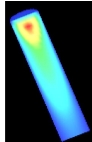
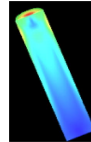
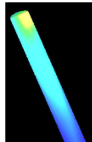
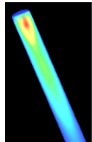
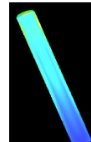
Based on the ZEMAX© and LASCAD© numerically optimized design parameters of the three-rod solar laser system in Section 3, a solar laser prototype was firstly designed and built in Lisbon in the first half of 2019, and then tested by both the PROMES-CNRS and the NOVA solar facilities during July – September 2019. Continuous-wave 1064 nm solar laser beams were successfully obtained from the three rods in both facilities, gaining more solar-to-laser conversion efficiency and accomplishing laser beam profiles measurements by the NOVA facility in the last weeks of September 2019.

As shown in Figs. 4 and 5, each 3 mm diameter, 25 mm length Nd:YAG rod was HR1064 nm coated

($R \geq 99.8\%$ @ 1064 nm) on one end face and AR1064 nm coated ($R \leq 0.2\%$ @ 1064 nm) on the other end face. To achieve maximum solar laser output power with enhanced beam brightness, each $R = 95\%$,

$RoC = \infty$ PR1064 nm mirror was mounted 50 mm away from the AR 1064 nm output face of each laser rod, as indicated in Fig. 3. By varying the rotation angle of the shutter, different input solar power and output laser power were respectively measured with a Molectron PowerMax 500D and a Thorlabs PM1100D power meters.

Table 1
Numerically calculated laser output performances of both the single-rod and the three-rod pumping schemes.

	Solar pump power absorption efficiency	Multimode solar laser power	Laser beam M^2 factors	Laser beam brightness figure of merit	Heat load	Temperature	Thermal stress
5.2 mm diameter, 25 mm length rod Single-rod scheme	44.8%	20.9 W	$M_x^2 = 32.1$ $M_y^2 = 32.1$	0.02 W			
3.0 mm diameter 25 mm length rods Three-rod scheme	40.1%	6.2 W for each rod 3×6.2 W = 18.6 W for three rods	$M_x^2 = 10.8$ $M_y^2 = 14.7$	0.039 W			
Comparison between three-rod and single-rod schemes	4.7% reduction	11% reduction	2.97 times reduction for M_x^2 2.18 times reduction for M_y^2	1.95 times Improvement	31.6% reduction	22 K reduction	65.5% reduction

Direct solar irradiance was measured simultaneously during the lasing process. It varied between 800 W/m² and

840 W/m². After considering all the shading effects in the primary concentrator, an effective collection area of 1.0 m² was adopted. For 830 W/m² solar irradiance, 620 W solar power was measured at the focus of the primary concentrator. As shown in Fig. 6, maximum multimode solar laser power of 18.3 W was successfully registered, corresponding to 18.3 W/m² collection efficiency. 6.1 W average solar laser power from each rod was hence obtained. Threshold solar pump power of 500 W was also measured, resulting in the solar laser slope efficiency of 5.1%.

5. Solar laser beam profile and its dependency on resonant cavity length and output coupler optical alignment

The laser beam M² quality factor of each laser rod at L = 50 mm was measured according to ISO 11146-1 standards, by using a CINOGY UV-NIR beam profiler - CinCam CMOS. The measured solar laser beam widths along the beam caustic, together with the extrapolated hyperbolic plot of the measured data, are given in Fig. 7. For the RoC = ∞ PR1064 nm mirror, M_x² = 11.0, M_y² = 15.3 were experimentally determined for one laser rod, leading to the beam brightness figure of merit of 0.036 W, being 9 times higher than that of the most efficient solar lasers with 32.5 W/m² collection efficiency (Liang et al., 2018).

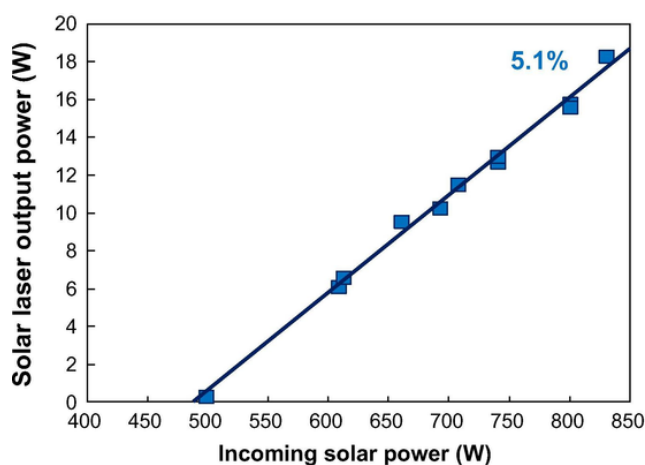


Fig. 6. Total solar laser output power from the three rods versus incoming solar power for R = 95%, RoC = ∞ and L₁ = L₂ = L₃ = 50 mm.

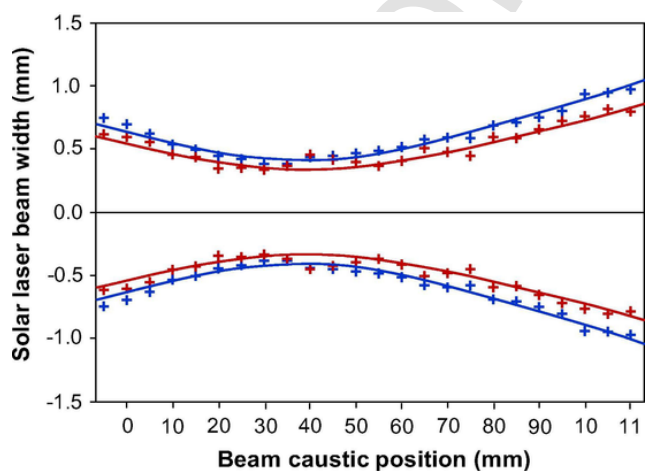


Fig. 7. Caustic fit measurements of the multimode solar laser beam from one of the three rods.

Different laser output beam profiles from the three laser rods were achieved by adjusting the PR mirrors of the solar laser resonant cavity. Fig. 8a indicates the output beam profiles with one sharp peak and two weak peaks when there were accurate laser resonant cavity alignment of the PR1064 nm mirror 3, while PR1064 nm mirror 1 and 2 were poorly aligned. 8.9 W total solar laser power was measured in this case. Fig. 8b shows different laser beam profiles with two strong peaks and one weak peak when the

PR1064 nm mirror 2 and 3 were well aligned and the PR1064 nm mirror 1 was not accurately aligned.

12.3 W total solar laser power was measured. When all the three PR1064 nm mirrors were accurately aligned with their respective laser rods, solar laser beam profiles with three sharp peaks were achieved, as shown in Fig. 8c. The maximum total solar laser power of 18.3 W was measured.

By choosing different laser resonant cavity lengths for the three rods, significantly different output laser beam profiles were achieved. As shown in Fig. 8d, a sharp peak from the rod 1 was observed with the resonator cavity length L₁ = 65 mm, while other two relatively weak peaks were observed from the rod 2 and 3 by adopting L₂ = 48 mm and L₃ = 56 mm, respectively. 15.4 W total solar laser power was measured. The simultaneous production of three laser beams with considerably different profiles may constitute an advantage for the three-rod solar laser scheme in finding more applications. Enhanced solar laser power could be achieved if PR1064 nm mirrors with small RoC were adopted. However, large M² factors would be measured, which inevitably would result in laser beams with reduced brightness figure of merit.

6. Conclusions

The three-rod Nd:YAG solar laser scheme was composed of the first-stage heliostat-parabolic mirror solar energy collection and concentration system, the second-stage fused silica aspheric lens and the third-stage conical-shaped pumping cavity, within which the three 3 mm diameter, 25 mm length Nd:YAG rods were efficiently pumped. Optimum optical pumping system design parameters were found through ZEMAX© software. Optimum solar laser power and beam parameters were found through LASCAD© numerical analysis. 18.3 W continuous-wave multimode total solar laser power was measured, corresponding to 5.1% system slope efficiency and 18.3 W/m² solar laser collection efficiency. 0.036 W laser beam brightness figure of merit was also obtained, being 9 times higher than that of the most efficient solar laser with 32.5 W/m² collection efficiency (Liang et al., 2018). By increasing the resonant cavity length from the AR1064nm laser rod end face, different solar laser output power and beam profiles were obtained for the three rods. Simultaneous solar laser emissions from the three 3 mm diameter rods could provide new solutions for solar-powered lasers applications.

7. Funding information

Financial support of the strategic project (UID/FIS/00068/2019) of the Science and Technology Foundation of Portuguese Ministry of Science, Technology and Higher Education (FCT - MCTES) is acknowledged. Financial support by the Solar Facilities for European Research Area -Third Phase (SFERA III), Grant Agreement No. 823802 is gratefully acknowledged.

Acknowledgment

FCT-MCTES grants SFRH/BPD/125116/2016, PD/BD/142827/2018, PD/BD/128267/2016 of C. R.Vistas, D. Garcia, B. D. Tibúrcio, respectively, and FCT-MCTES Junior Researcher Contract CEECIND/03081/2017 of J. Almeida are acknowledged.

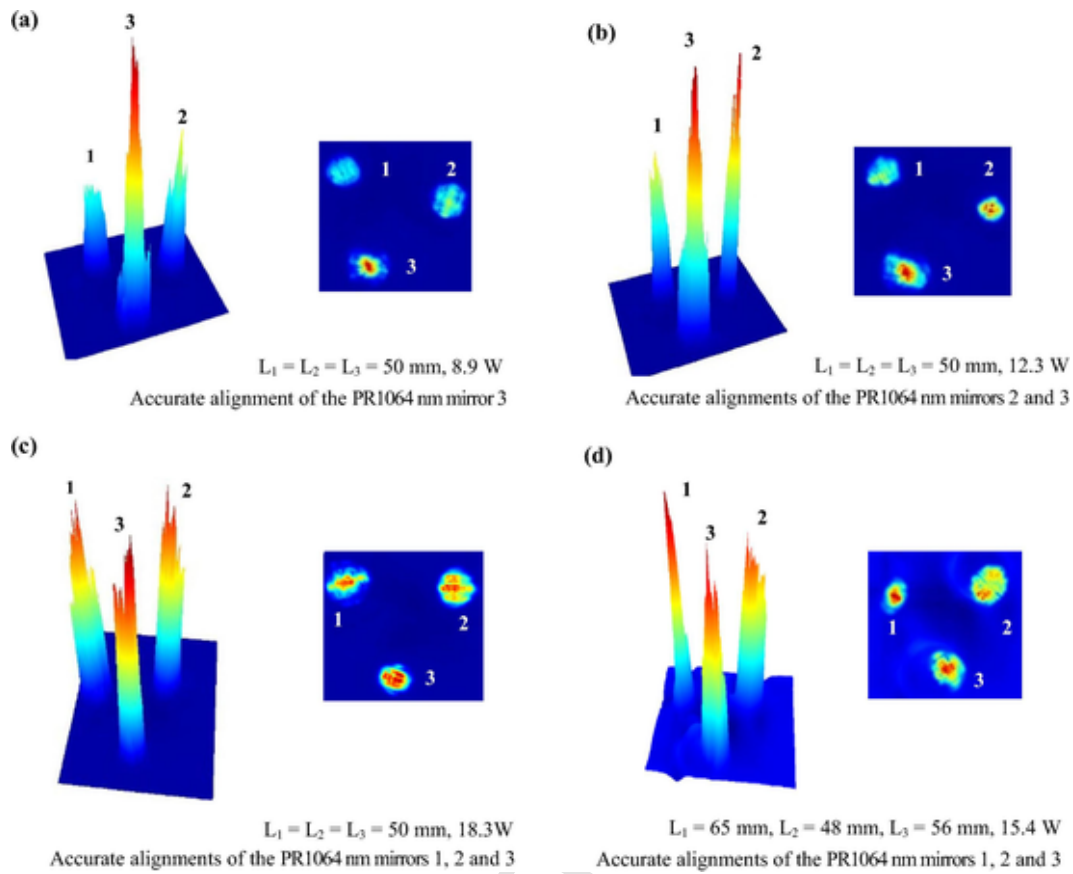


Fig. 8. Measured output laser beam 3D and 2D profiles of the three-rod laser system at different resonant cavity alignments and lengths.

References

- Almeida, J., Liang, D., Guillot, E., Abdel-Hadi, Y., 2013. A 40 W cw Nd:YAG solar laser pumped through a heliostat: a parabolic mirror system. *Laser Phys.* 23, 065801–065801.
- Arashi, H., Oka, Y., Sasahara, N., Kaimai, A., Ishigame, M., 1984. A solar-pumped cw 18 W Nd:YAG laser. *Jpn. J. Appl. Phys.* 23, 1051–1053.
- Benmair, R.M.J., Kagan, J., Kalisky, Y., Noter, Y., Oron, M., Shimony, Y., Yogeve, A., 1990. Solar-pumped Er, Tm, Ho: YAG laser. *Opt. Lett.* 15, 36–38.
- Bruening, S., Du, K., Jarczynski, M., Jenke, G., Gillner, A., 2018. Ultra-fast laser micro processing by multiple laser spots. *Procedia CIRP* 74, 573–580.
- Dinh, T.H., Ohkubo, T., Yabe, T., Kuboyama, H., 2012. 120 watt continuous wave solar-pumped laser with a liquid light-guide lens and a Nd:YAG rod. *Opt. Lett.* 37, 2670–2672.
- Guan, Z., Zhao, C., Yang, S., Wang, Y., Ke, J.Y., Zhang, H., 2017. Demonstration of a free-space optical communication system using a solar-pumped laser as signal transmitter. *Laser Phys. Lett.* 14 (5), 55804.
- Lando, M., Kagan, J., Linyekin, B., Dobrusin, V., 2003. A solar pumped Nd:YAG laser in the high collection efficiency regime. *Opt. Commun.* 222, 371–381.
- Liang, D., Almeida, J., 2011. Highly efficient solar-pumped Nd:YAG laser. *Opt. Exp.* 19, 26399–26405.
- Liang, D., Almeida, J., Vistas, C.R., Guillot, E., 2017. Solar-pumped Nd:YAG laser with 31.5 W/m^2 multimode and 7.9 W/m^2 TEM₀₀-mode collection efficiencies. *Sol. Energy Mat. Sol. Cells* 159, 435–439.
- Liang, D., Vistas, C.R., Tíbúrcio, B.D., Almeida, J., 2018. Solar-pumped Cr:Nd:YAG ceramic laser with 6.7% slope efficiency. *Sol. Energy Mat. Sol. Cells* 185, 75–79.
- Strite, T., Gusenko, A., Grupp, M., Hout, T., 17th, 2016. Fiber lasers: Multiple laser beam material processing. *Laser Focus World*, Feb..
- Vasile, M., Maddock, C.A., 2012. Design of a formation of solar pumped lasers for asteroid deflection. *Adv. Space Res.* 50 (7), 891–905.
- Weksler, M., Shwartz, J., 1988. Solar-pumped solid-state lasers. *IEEE J. Quantum Electron.* 24, 1222–1228.
- Yabe, T., Ohkubo, T., Uchida, S., Nakatsuka, M., Funatsu, T., Mabuti, A., Oyama, A., Nakagawa, Y., Oishi, T., Daito, K., Behgol, B., Nakayama, Y., Yoshida, M., Motokoshi, S., Sato, Y., Baasandash, C., 2007. High efficiency and economical solar energy pumped laser with Fresnel lens and chromium co-doped laser medium. *Appl. Phys. Lett.* 90, 261120–261123.
- Young, C.G., 1966. A sun pumped cw one-watt laser. *Appl. Opt.* 5, 993–997.